Electromechanical response of single-walled carbon nanotubes to torsional strain in a self-contained device

ADAM R. HALL[1], MICHAEL R. FALVO[1,2], RICHARD SUPERFINE[1,2,3] AND SEAN WASHBURN[1,2,3,4]*

[1]Curriculum in Applied and Materials Sciences; [2]Department of Physics and Astronomy; [3]Department of Computer Science; [4]Department of Biomedical Engineering, University of North Carolina at Chapel Hill, Chapel Hill, North Carolina 27599, USA
*e-mail: sean@physics.unc.edu

Nanoscale electronics seeks to decrease the critical dimension of devices in order to improve performance while reducing power consumption. Single-walled carbon nanotubes fit well with this strategy because, in addition to their molecular size, they demonstrate a number of unique electronic, mechanical and electromechanical properties. In particular, theory[1–8] predicts that strain can have a large effect on the band structure of a nanotube, which, in turn, has an influence on its electron transport properties. This has been demonstrated in experiments where axial strain was applied by a scanning probe[9–12]. Theory also predicts that torsional strain can influence transport properties, which was observed recently in multiwalled nanotubes[13]. Here we present the first experimental evidence of an electromechanical effect from torsional strain in single-walled nanotubes, and also the first measurements of piezoresistive response in a self-contained nanotube-based nanoelectromechanical structure.

The system we use to examine the effect of torsional strain[14] consists of an individual single-walled nanotube (SWNT) suspended between two metal structures (anchors) and supporting a smaller metal platform (or paddle) at its centre (Fig. 1). Similar devices have been demonstrated previously[15–19] for a range of purposes, including the direct measurement of SWNT shear (twisting) modulus[20]. The fabrication of our devices follows the methods given in the earlier work, with special care taken to ensure good electrical contact. Briefly, SWNTs were grown by a chemical vapour deposition method[21] onto a degenerately doped silicon wafer with a 1-μm thermal oxide layer. The growth method has been shown to result in SWNTs of average diameter 0.97 nm as measured by atomic force microscopy[20]. Photolithography to define macroscopic contact leads was followed by electron-beam lithography (EBL) to position the anchors and paddle along the length of an SWNT. Devices were then subjected to a 400 °C anneal under argon to decompose excess residues between the nanotube and the metal contacts. This was followed by a final EBL step in which windows were defined in the electron beam resist over the paddles. A wet chemical etch with buffered hydrofluoric acid was then used to remove oxide from beneath the paddles. Finally, samples were dried in supercritical CO_2.

Device actuation was performed electrostatically with a voltage bias between the underlying silicon substrate (backgate) and the structure above. The voltage induced dipolar attraction between the surfaces of the suspended paddle and the substrate. Asymmetries inherent in the fabrication process led to a net torque on and rotation of the paddle and hence to torsional strain in the SWNT. The paddles were thick in comparison with their lengths, which places the centroid of the paddle well above the nanotube axis. This allows electrostatic deflection up to nearly π radians (Fig. 1b) rather than the $\pi/2$ radians attained by previous devices[20].

Recent work has focused on transport effects in similar devices built with multiwalled nanotubes (MWNTs) and twisted with a scanning probe tip[13]. However, this work assumed transport only through the outer shell, which may or may not be the case. The use of SWNTs simplifies the system by removing the complexities of multiple shells. Furthermore, the use of electrostatic forces for actuation removes perturbations (electrical potential, changes in point of contact, and so on) that may be caused by direct mechanical contact with a probe, and allows the system to be entirely self-contained. These are the first measurements to feature such autonomy, which is important for potential applications.
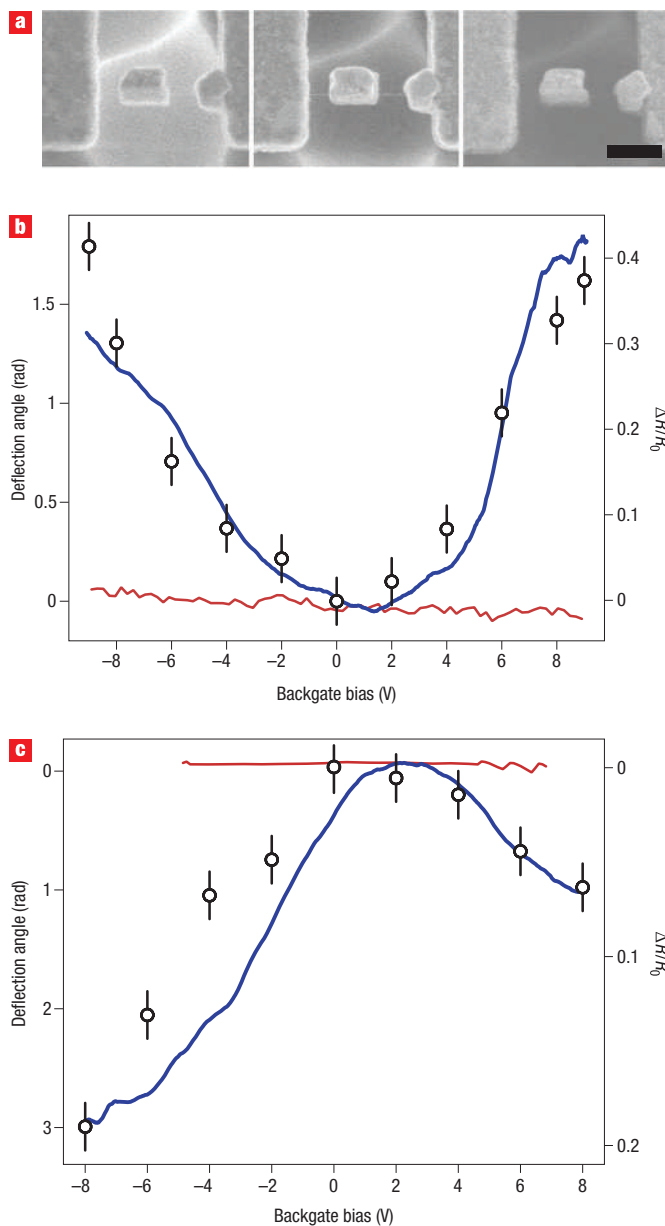
All experiments were performed *in situ* in a scanning electron microscope (Hitachi S-4700), which allowed visual verification of the actuation (Fig. 2a). We found that electrical measurements were affected by imaging, perhaps owing to contamination, and we therefore performed these measurements before electron-beam exposure. Device deflection was measured from the length of the paddle image relative to its initial length for each applied backgate voltage[20], giving us the relation between bias and angle (Fig. 2b,c).

The electrical measurement is shown in Fig. 1c. Source−drain transport properties were monitored while a varying actuation bias was applied to the backgate electrode. We note that the application of either positive or negative bias to the backgate results in a net torque in the same direction and thus the same strain in the SWNT. This allows us to separate the torsional response of the rather short twisting sections of the SWNT from any field effect (transconductance) in the much longer static

413
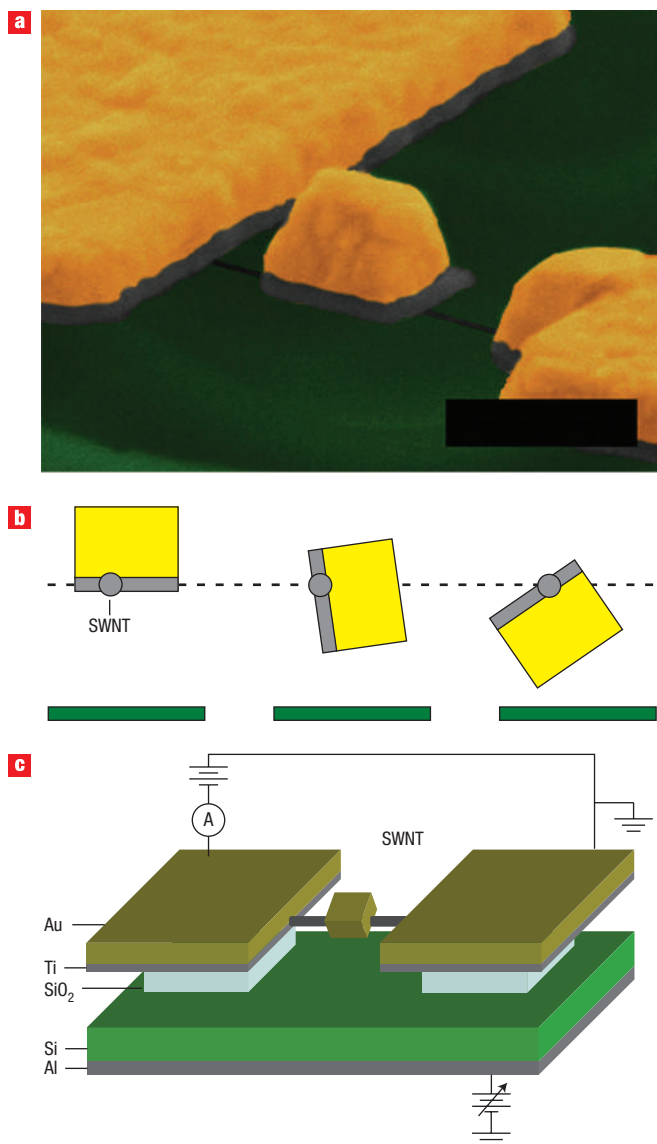
Figure 1 The SWNT torsional device. a, A false-colour scanning electron micrograph of an SWNT torsional device (scale bar = 500 nm). **b**, Diagram demonstrating rotation of nearly π radians of a thick paddle (backgate bias voltage increases left to right). **c**, Schematic diagram of the transport versus strain measurement.

Figure 2 Actuation and electromechanical response of two SWNT torsional devices. a, Scanning electron micrographs of a typical device under backgate voltages −9, 0 and 9 V, respectively (scale bar = 500 nm). (See Supplementary Information for video of this actuation.) **b,c**, Measured paddle deflection (open circles) and differential resistance both before (red) and after (blue) etching versus backgate voltage for a device demonstrating a positive (**b**) and a negative (**c**) relation between resistance and deflection.

sections, which should be monotonic in the applied backgate voltage. We also note that any field effect on the etched device would be expected to be smaller even than the dependence measured prior to etching, given the low dielectric constant of the vacuum gap separating the device from the underlying substrate. Figure 2b,c shows the size of the response before and after the etching step. Before etching the response appears to be due solely to field effects. The response is slightly n-type, likely due to band bending at the nanotube–metal junction barriers[22,23], although p-type behaviour of similar size has been seen in other devices. Taking into account the large (1 μm) oxide thickness and probable surface states on the free surface of the oxide, we expect a small field effect. No device has demonstrated symmetry about 0 V prior to etching. After etching, the response follows the deflection of the paddle as expected for the

electromechanical effect. The measured resistances, R_0, after etching were typically tens of MΩ. Similar dependences on torsion were observed using both high and low source–drain bias, the high bias (1–7 V) measurements being made in regions below current saturation from optical phonons[24].

We now analyse the effect of torsional strain on SWNT transport properties. Figure 3 shows results from several SWNT torsional devices. Using the relation between applied backgate bias and deflection angle for each device, we correlated the measured deflection to SWNT torsional strain γ through the
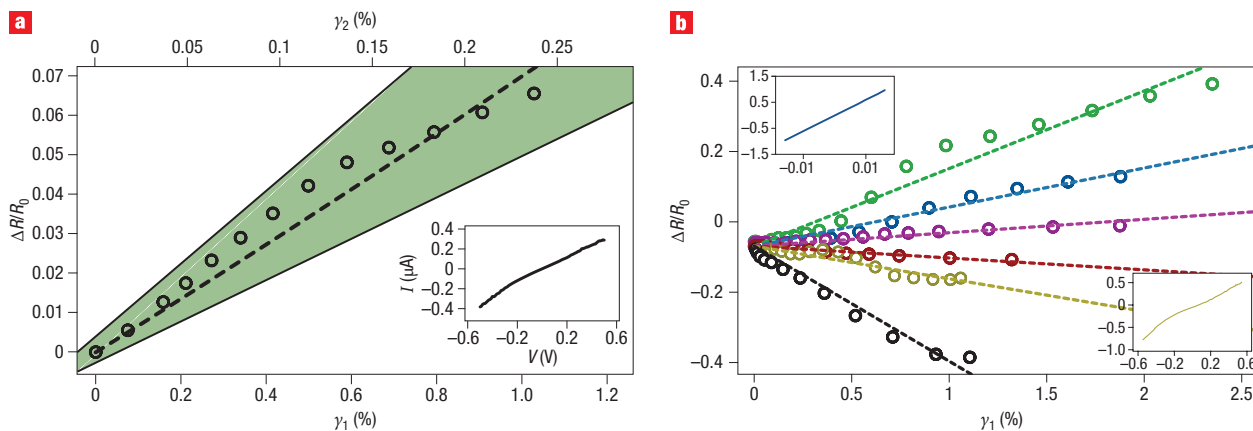
Figure 3 Characterization of SWNT transport properties under applied torsional strain. a, Differential resistance versus SWNT torsional strain for a typical device taken at low source–drain bias. γ_1 and γ_2 are the strains in the sections of the nanotube to the left and right of the paddle, respectively. The dashed line is a fit to equation (4), and the shaded region represents the total measurement error. Insets: source–drain I–V characteristics of the SWNT prior to etching. After etching, measured resistance (R_0) for this device was 54 MΩ in the linear region. **b**, Relation between SWNT differential resistance and torsional strain (shorter side only) for six additional devices, demonstrating the range of observed responses. Insets: I–V characteristics for two typical devices (colour indicated), one showing increasing resistance and one showing decreasing resistance.

equation $\gamma = (r\theta)/l$, where r is the nanotube radius and l is nanotube length. For these samples, no reliable measurement of the radius could be made after etching, so we assume a value equal to the average radius for SWNT grown with our CVD method (0.49 nm). By including a variation of 20%, we statistically account for about 95% of all nanotubes present on the sample[20]. The two strains plotted in Fig. 3a (γ_1 and γ_2) represent the section of SWNT to the left and right of the paddle, respectively, as the lengths l_1 and l_2 were unequal. For this device, $l_1 = 163 \pm 16$ nm and $l_2 = 564 \pm 56$ nm. No device demonstrated any dependence on backgate sweep direction.

Figure 3b shows responses for six additional devices. Actuation caused an increase in SWNT resistance for half of these devices, in which the torsional strain opens the gap in this SWNT. Measured I–V characteristics (top inset) varied in these devices, ranging from metallic (depletion mode) to semiconducting. In contrast, the resistance was decreased in the other devices, indicating a smaller gap under strain as is typical for semiconducting SWNTs. Importantly, all devices demonstrating this decrease in resistance show some nonlinearity in their measured I–V characteristics, indicating semiconducting characteristics.

We explain this behaviour through a relationship between SWNT bandgap (E_g) and the strains applied to it[5]. For our system, we expect the bandgap to change with torsional strain as

$$\frac{dE_g}{d\gamma} = \text{sgn}(2p+1)3t_o \sin 3\phi(m,n) \qquad (1)$$

where t_o is the tight-binding overlap integral (2.7 eV), $\phi(m,n)$ is the nanotube chiral angle, m and n are the lattice indices of the SWNT, and $p = -1$, 0 or 1 such that it satisfies the relation $n - m = 3q + p$, where q is an integer. For all metallic nanotubes ($p = 0$) and half of all semiconducting nanotubes ($p = 1$), application of torsional strain will result in the creation or increase of the bandgap ($dE_g/d\gamma > 0$). For other semiconducting SWNTs ($p = -1$), the bandgap will be decreased for the same strain ($dE_g/d\gamma < 0$).

We viewed devices from an oblique angle while applying the gate bias, and no measurable vertical displacement of the nanotube or paddle was observed. The axial displacement cannot be greater than the resolution of these images, and we infer an upper bound of 0.1% axial strain. As this level of strain resulted in a very small resistance change in all previous studies[10–12], we consider the axial component negligible.

We expect the nanotube resistance to vary with the gap according to[11]

$$R_{NT} = \frac{1}{|t|^2}\frac{h}{8e^2}\left(1 + \exp\left(\frac{E_o + \gamma(dE_g/d\gamma)}{kT}\right)\right) \qquad (2)$$

where $|t|^2$ is the probability of electron transmission across the band gap, E_o is the unstrained band gap and kT is the thermal energy. Thus, our observation of both increase and decrease on different devices is expected and is supported by the measured I–V characteristics.

Changes in details of the contact between the nanotube and the metal lead during deflection can cause resistance changes, but such changes are difficult to predict in detail. Electrostatically induced deformations at the nanotube–metal interface, in general, will bend the tube down (toward the substrate). Because these devices are built from SWNTs buried under deposited metal leads, such deformation will tend to pull the nanotube out of contact with the metal and thus to increase resistance. Moreover, we have observed no response in devices with long torsional springs where the torsional strain was too low, but where the contacts were still subject to similar local stresses.

The total measured resistance of the system is

$$R_T = R_C + R_{NT1} + R_{NT2} \qquad (3)$$

where R_C is the contact resistance of the metal leads to the nanotube, and R_{NT1} and R_{NT2} are the resistance contributions of each supporting section of SWNT. Combining equations (1), (2) and (3), we arrive at a relation between the change in

resistance of the device and the torsional strains in the section of nanotube:

$$\frac{\Delta R_T(\gamma)}{R_o} = \frac{R_C + R_{NT}(+\gamma_1) + R_{NT}(-\gamma_2)}{R_C + 2R_{NT}(0)} - 1 \qquad (4)$$

We note that the strain on one side of the paddle will tend to compensate the response from the section on the other side. Because equation (2) is intended for low source–drain bias measurements, we fit the data shown in Fig. 3a (lock-in measurement, amplitude 50 mV) to this equation. In principle, we can gain further insight into the nanotube structure. The change in resistance due to etching was $10\,M\Omega$ (after etching, the measured resistance was $14\,M\Omega$), which we attribute to a decrease in contact between the SWNT and the metal leads. Because the measured resistances of the nanotubes before etching were much lower, we consider the change to be an estimate of the total contact resistance R_C. We then fit to the remaining parameters of $|t|^2$, E_o and $\phi(m, n)$. We find that the presented SWNT fits best with an initial bandgap energy of 29 meV and an estimated chiral angle ϕ of $\sim 57°$. Errors in our measurement, especially in that of the nanotube radius, prevent high accuracy for this value. The fit agrees with a transmission probability of 0.2, in agreement with other SWNT devices[11,12]. However, varying this parameter over a large range did not affect the other values significantly, demonstrating its high uncertainty.

These self-contained nanoelectromechanical torsional devices allow repeated application of torsional strain to individual SWNTs that are components of an electrical circuit. By measuring their strain while simultaneously measuring their transport properties, we have demonstrated that added strain can increase the resistance of some nanotubes but decrease the resistance of others. We attribute the effect to the increase or decrease in bandgap of the particular SWNT as dictated by its particular chiral structure. These are the first direct measurements of a torsion–transport relation in SWNTs and the first measurements of an electromechanical response in an autonomous NEMS structure based on individual SWNTs.

References

1. Heyd, R., Charlier, A. & McRae, E. Uniaxial-stress effects on the electronic properties of carbon nanotubes. *Phys. Rev. B* **55,** 6820–6824 (1997).
2. Kane, C. L. & Mele, E. J. Size, shape, and low energy electronic structure of carbon nanotubes. *Phys. Rev. Lett.* **78,** 1932–1935 (1997).
3. Rochefort, A., Avouris, P., Lesage, F. & Salahub, D. R. Electrical and mechanical properties of distorted carbon nanotubes. *Phys. Rev. B* **60,** 13824–13830 (1999).
4. Yang, L., Anantram, M. P., Han, J. & Lu, J. P. Band-gap change of carbon nanotubes: Effect of small uniaxial and torsional strain. *Phys. Rev. B* **60,** 13874–13878 (1999).
5. Yang, L. & Han, J. Electronic structure of deformed carbon nanotubes. *Phys. Rev. Lett.* **85,** 154–157 (2000).
6. Maiti, A., Svizhenko, A. & Anantram, M. P. Electronic transport through carbon nanotubes: Effects of structural deformation and tube chirality. *Phys. Rev. Lett.* **88,** 126805 (2002).
7. Ding, J. W. *et al.* Curvature and strain effects on electronic properties of single-wall carbon nanotubes. *J. Phys. Condens. Matter* **15,** L439–L445 (2003).
8. Guo, G. Y., Liu, L., Chu, K. C., Jayanthi, C. S. & Wu, S. Y. Electromechanical responses of single-walled carbon nanotubes: Interplay between the strain-induced energy-gap opening and the pinning of the Fermi level. *J. Appl. Phys.* **98,** 044311 (2005).
9. Tombler, T. W. *et al.* Reversible electromechanical characteristics of carbon nanotubes under local-probe manipulation. *Nature* **405,** 769–772 (2000).
10. Cao, J., Wang, Q. & Dai, H. J. Electromechanical properties of metallic, quasimetallic, and semiconducting carbon nanotubes under stretching. *Phys. Rev. Lett.* **90,** 157601 (2003).
11. Minot, E. D. *et al.* Tuning carbon nanotube band gaps with strain. *Phys. Rev. Lett.* **90,** 156401 (2003).
12. Stampfer, C. *et al.* Nano-electromechanical displacement sensing based on single-walled carbon nanotubes. *Nano Lett.* **6,** 1449–1453 (2006).
13. Cohen-Karni, T., Segev, L., Srur-Lavi, O., Cohen, S. R. & Joselevich, E. Torsional electromechanical quantum oscillations in carbon nanotubes. *Nature Nanotech.* **1,** 36–41 (2006).
14. Williams, P. A. *et al.* Fabrication of nanometer-scale mechanical devices incorporating individual multiwalled carbon nanotubes as torsional springs. *Appl. Phys. Lett.* **82,** 805–807 (2003).
15. Williams, P. A. *et al.* Torsional response and stiffening of individual multiwalled carbon nanotubes. *Phys. Rev. Lett.* **89,** 255502 (2002).
16. Fennimore, A. M. *et al.* Rotational actuators based on carbon nanotubes. *Nature* **424,** 408–410 (2003).
17. Bourlon, B., Glattli, D. C., Miko, C., Forro, L. & Bachtold, A. Carbon nanotube based bearing for rotational motions. *Nano Lett.* **4,** 709–712 (2004).
18. Papadakis, S. J. *et al.* Resonant oscillators with carbon-nanotube torsion springs. *Phys. Rev. Lett.* **93,** 146101 (2004).
19. Meyer, J. C., Paillet, M. & Roth, S. Single-molecule torsional pendulum. *Science* **309,** 1539–1541 (2005).
20. Hall, A. R. *et al.* Experimental measurement of single-wall carbon nanotube torsional properties. *Phys. Rev. Lett.* **96,** 256102 (2006).
21. Li, Y., Liu, J., Wang, Y. Q. & Wang, Z. L. Preparation of monodispersed Fe-Mo nanoparticles as the catalyst for CVD synthesis of carbon nanotubes. *Chem. Mat.* **13,** 1008–1014 (2001).
22. Martel, R. *et al.* Ambipolar electrical transport in semiconducting single-wall carbon nanotubes. *Phys. Rev. Lett.* **87,** 256805 (2001).
23. Javey, A., Shim, M. & Dai, H. J. Electrical properties and devices of large-diameter single-walled carbon nanotubes. *Appl. Phys. Lett.* **80,** 1064–1066 (2002).
24. Javey, A. *et al.* High-field quasiballistic transport in short carbon nanotubes. *Phys. Rev. Lett.* **92,** 106804 (2004).

Author contributions

A.R.H. designed and performed the experiments and fabricated the devices. Data analysis was peformed by A.R.H. with S.W. All authors discussed results and commented on the manuscript.